# Improvement of oncolytic adenovirus vectors through genetic capsid modifications

Vrij, J. de

# CHAPTER 4

## ADENOVIRUS TARGETING TO HLA-A1/MAGE-A1-POSITIVE TUMOR CELLS BY FUSING A SINGLE-CHAIN T-CELL RECEPTOR WITH MINOR CAPSID PROTEIN IX

J de Vrij[1], TG Uil[1], SK van den Hengel[1], SJ Cramer[1], D Koppers-Lalic[1], MC Verweij[2], EJHJ Wiertz[2], J Vellinga[1], RA Willemsen[3], and RC Hoeben[1]

[1]Department of Molecular Cell Biology and [2]Department of Medical Microbiology, Leiden University Medical Center, Leiden, The Netherlands and [3]Tumor Immunology Group, Unit of Clinical and Tumor Immunology, Department of Medical Oncology, Erasmus MC-Daniel den Hoed, Rotterdam, The Netherlands

Gene Therapy 2008;15:978-989

## ABSTRACT

Adenovirus vectors have great potential in cancer gene therapy. Targeting of cancer-testis (CT) antigens, which are specifically presented at the surface of tumor cells by human leukocyte antigen (HLA) class I molecules, is an attractive option. In this study, a single-chain T-cell receptor (scTCR) directed against the CT antigen melanoma-associated antigen (MAGE)-A1 in complex with the HLA class I molecule of haplotype HLA-A1, is fused with the C-terminus of the adenovirus minor capsid protein IX. Propagation of a protein-IX (pIX)-gene-deleted human adenovirus-5 (HAdV-5) vector on cells that constitutively express the pIXscTCR fusion protein yielded viral particles with the pIXscTCR fusion protein incorporated in their capsid. Generated particles specifically transduced melanoma cell lines expressing the HLA-A1/MAGE-A1 target complex with at least ten-fold higher efficiency than control viruses. Whereas loading of HLA-A1 positive cells with MAGE-A1 peptides leads to enhanced transduction of the cells, the efficiency of virus transduction is strongly reduced if the HLA-A1 molecules are not accessible at the target cell. Taken together, these data provide proof-of-principle that pIXscTCR fusions can be used to target HAdV-5 vectors to tumor cells expressing intracellular CT antigens.

# INTRODUCTION

Recombinant viral vectors hold great promise in the field of cancer gene therapy. Much effort is devoted to generating vectors that have the ability to specifically transduce tumor cells. In this respect it will be of major interest to develop vectors that are targeted to antigens that are specifically expressed at the surface of tumor cells to prevent transduction of noncancerous cells.

Intriguingly, in many cases cancer cells have been found to induce a tumor cell-specific response of the immune system. Cytotoxic T lymphocytes (CTLs) have been discovered that eradicate tumor cells via the recognition of tumor-specific antigens, while leaving healthy tissue intact. Such tumor-specific antigens might belong to the group of so-called 'cancer-testis' (CT) antigens, which are presented at the tumor cell surface by major histocompatibility complex (MHC) class I molecules that are recognized by CTLs.[1] CT antigens are expressed in a variety of cancerous tissues and are generally silent in normal tissues, except for the testis.[2] To date, 89 CT genes or isoforms, which are organised into 44 families, have been described. From these, 19 families are testis restricted, 11 show additional expression in one or two somatic tissues, 9 are expressed in three to six tissue types besides testis and 5 are ubiquitously somatically expressed. With the exception of the testis-restricted CT antigens, the others also show expression in the pancreas but at levels as much as 10 times lower than in the testis.[2] Expression of CT antigens was first shown in melanoma and all the classic CT antigens are expressed in this type of tumor, but since the 1980s, expression in various other tumors has been recognised.[2] The highly specific expression profiles of the CT antigens make them interesting target molecules for cancer therapies. Importantly, CT antigens belonging to the melanoma-associated antigen (MAGE) A, B and C family seem to be involved in oncogenesis, providing protection against apoptosis in tumor cells.[3] The expression of other tumor antigens, such as 'overexpression' antigens p53 and HER-2/neu, or 'differentiation antigens' gp100 and Mart-1, is less restricted to tumor cells and their use for cancer-drug targeting may be associated with negative side effects.

The principle of targeting human MHC class I molecules (human leukocyte antigen, HLA class I), in complex with tumor-specific antigens, has been the subject of many studies on T-cell targeting to tumor cells.[4] So far, HLA class I/peptide targeting of viral vectors has not been extensively explored. Promising results have been obtained by targeting measles virus particles to a specific HLA class I/peptide complex via fusion of a single-chain T-cell receptor (scTCR) to the attachment protein H of the virus.[5] Recently, adenovirus has been also retargeted to CT antigens by replacing the knob domain of the fiber protein with a CT antigen-specific scTCR.[6]

Adenoviral vectors are among the most promising viral vectors for cancer gene therapy for several reasons. They can be produced in large quantities, they do not lead to stable genetic modification of the transduced cells and they have a good safety profile.[7] Genetic modification of adenoviral capsid proteins might lead to the development of vectors that are specifically targeted to tumor cells, thereby improving safety and efficacy. Cell binding of subgroup C-derived human adenovirus (HAdV) vectors (including HAdV-5 and HAdV-2), which are widely used in gene therapy, involves two distinct steps. First, they bind with high affinity to the coxsackie virus

and adenovirus receptor (CAR) at the cell surface. Second, interaction of penton base Arg-Gly-Asp (RGD) motifs with cellular integrins, including αvβ3 and αvβ5 leads to endocytosis.[8] Many tumor cells are relatively refractory to infection by subgroup C-derived HAdV vectors due to the paucity of CAR receptors.[9] Development of genetically modified vectors that can infect CAR-negative cells has mainly focused on incorporation of heterologous ligands in the fiber knob, or on replacement of the entire knob domain by a heterologous ligand.[7] The complexity of incorporating ligands into the adenovirus fiber locale has prompted the identification of other capsid proteins amendable for ligand incorporation. These approaches have the potential to incorporate an increased number of complex ligands per virion. To date, the capsid proteins hexon,[10,11] penton base,[12] minor capsid protein IX (pIX),[13-18] and protein pIIIa[19] have been explored as platforms for the incorporation of heterologous peptides (reviewed by Vellinga *et al.*[20]).

We have been exploiting the adenovirus minor capsid pIX as an anchor to genetically incorporate large proteins.[17,18] Protein IX is a small (14.3 kDa) protein of unknown structure that acts as capsid cement, stabilizing the interactions between hexon trimers on each facet of the virion.[21] Twelve molecules of pIX are associated with each facet of the icosahedron, with an overall stoichiometry of 240 pIX monomers per virion.[22] Although the main mass of pIX is thought to be located in the cavities between the so-called group-of-nine hexon capsomers, the postulated position of pIX in the capsid is being challenged.[23-26]

Nevertheless, we have recently demonstrated efficient and functional incorporation of the hyperstable single-chain antibody fragment 13R4 that was fused with pIX via a 75-Angstrom spacer.[18] The 13R4 was functional in the capsid as was evidenced by its capacity to bind *Escherichia coli* β-galactosidase.

Here we report the production of an adenoviral vector which is targeted to tumor cells presenting peptides of the CT antigen MAGE-A1 on HLA class I molecules of haplotype HLA-A1, via a scTCR ($TCR^{A1M1}$) fused with adenovirus minor capsid pIX. To ensure enhanced protrusion of the scTCR at the virus surface, a 75-Angstrom α-helical spacer was included between pIX and the TCR.[17] We produced virus particles that were efficiently loaded with the pIX_$TCR^{A1M1}$ fusion protein. The transduction efficiency of the HLA-A1/MAGE-A1-positive melanoma cell lines MZ2-MEL3.0 and MZ2-MEL43 was strongly increased upon incorporation of the fusion protein. These findings represent (1) the first demonstration of a pIXscTCR-mediated adenovirus targeting of a cell type that is normally refractory to HAdV-5, and (2) further proof-of-principle of targeting the highly tumor-specific CT antigen/HLA class I complexes at the surface of human tumor cell lines.

## RESULTS

### Establishment and characterization of the pIX_$TCR^{A1M1}$ producing helper cell line

To establish a helper cell line stably expressing the pIX_$TCR^{A1M1}$ fusion protein, 911 cells were transduced with the recombinant lentivirus LV.pIX_$TCR^{A1M1}$. A schematic

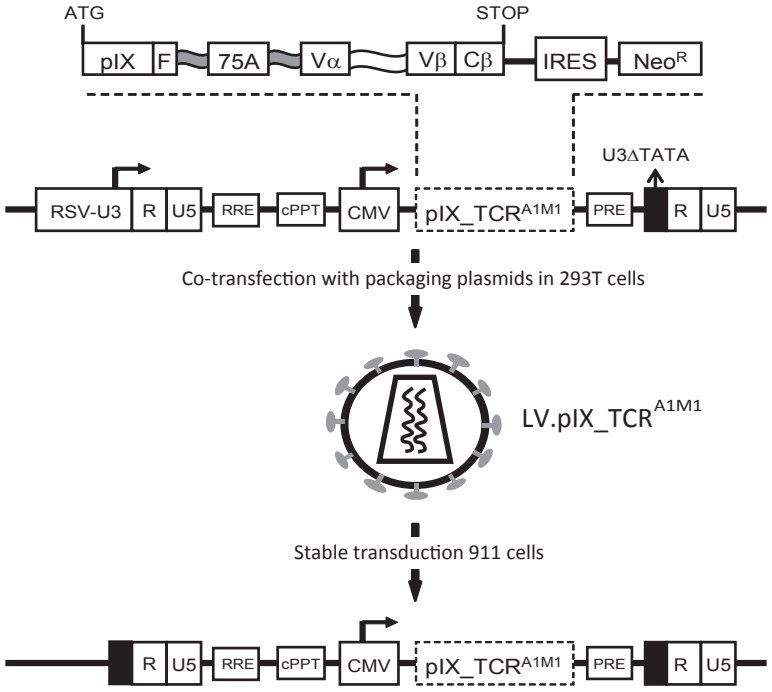


**Figure 1.** Schematic representation of the lentivirus system, used to establish the 911 helper cell line stably expressing pIX_TCR$^{A1M1}$. The vector used in this study is a third-generation, self-inactivating (SIN) vector, with major part of the 3' U3 region deleted, including the TATA box.[27] The Rev-responsive element (RRE),[28] the central polypurine tract (cPPT)[29-31] and the human hepatitis B virus-derived posttranscriptional regulatory element (PRE) are indicated. The encephalomyocardin virus internal ribosomal entry site (IRES) was obtained from pTM3.[32] The NPTII coding region (Neo$^R$), which mediates resistance to G418, was isolated from peGFPn2 (Clontech, Leusden, the Netherlands).

overview of the pro-lentiviral DNA construct and the sequence eventually incorporated in the 911 genome is provided in **Fig. 1**.

After growing the cells for several weeks in selection medium (containing 200 μg ml$^{-1}$ G418), western analysis on cell lysate was performed. This revealed pIX_TCR$^{A1M1}$ protein amounts that were similar to the pIX level in 911 cells infected with HAdV-5.LUC virus (**Fig. 2a**). The protein size of pIX_TCR$^{A1M1}$ was as expected (65.8 kDa). The percentage of pIX_TCR$^{A1M1}$-positive cells was determined by immunohistochemistry analysis (**Fig. 2b**). This showed more than 90% of the cells to be positive for pIX_TCR$^{A1M1}$. The pIX fusion protein appeared to be located mainly in the cytoplasm. Surprisingly, visualizing pIX_TCR$^{A1M1}$ protein in the cells by using a conformation-dependent antibody recognizing the variable domain of the scTCR (Vα12.1) was dependent on adenovirus infection of the cells (**Fig. 2c**). At 24 h post infection, a Vα12.1-mediated signal could be observed. Cells were infected with the viral vector HAdV-5.CMVLUCΔE1ΔE3ΔpIX (see next paragraph). Detection of pIX_scTCR$^{A1M1}$ by Vα12.1 antibody was absent at earlier time points of infection and in pIX_TCR$^{A1M1}$-

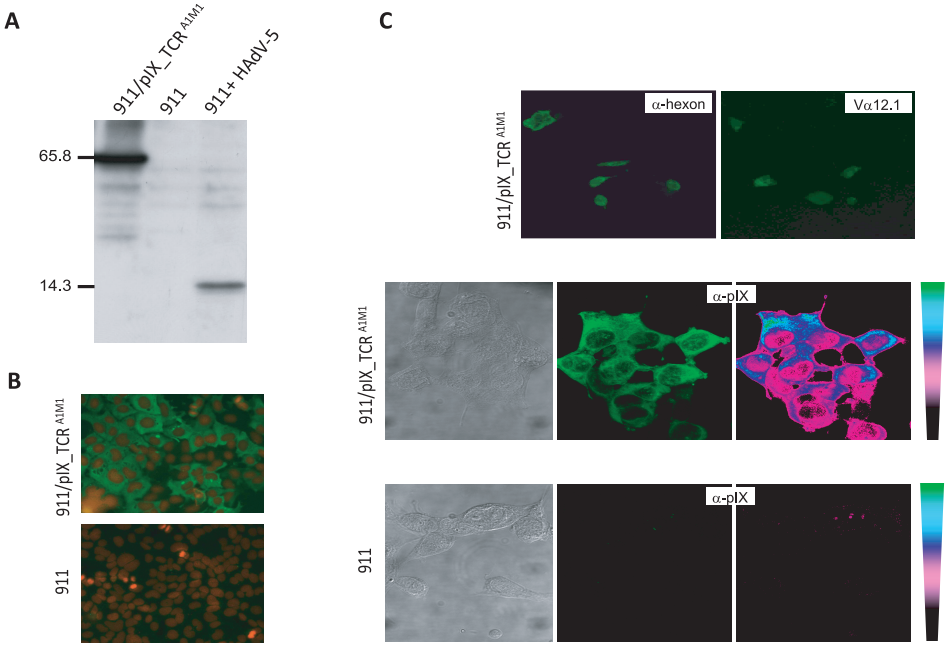


**Figure 2.** Characterization of the 911/pIX_TCR$^{A1M1}$ helper cell line. (**a**) Western analysis on lysates of the 911/pIX_TCR$^{A1M1}$ cells. Production of pIX_TCR$^{A1M1}$ was compared to the production of wild-type (wt) pIX in 911 cells infected with HAdV-5. Used antibodies were anti-pIX and horseradish peroxidase (HRP)-conjugated secondary antibody. The predicted size of 14.3 kDa for wt pIX and 65.8 kDa for pIX_scTCR$^{A1M1}$ was confirmed by the SDS–polyacrylamide gel electrophoresis (PAGE), as indicated in the figure. (**b**) Immunohistochemistry assay on 911/pIX_TCR$^{A1M1}$ cells. The pIX_TCR$^{A1M1}$ was visualized by using anti-pIX antibody. The nuclei were stained with propidium iodide. (**c**) Immunohistochemistry assays on 911/pIX_TCR$^{A1M1}$ cells, infected with HAdV-5ΔpIX. Fixation was performed at 24 h postinfection. The upper panel shows wide-field microscopy images of anti-hexon and Vα12.1-stained cells. The lower panel shows confocal microscopy images of anti-pIX-stained 911/pIX_TCR$^{A1M1}$. Infected 911 cells were included as negative control. To illustrate the presence of fluorescence signal in the nuclei more clearly, pseudocolor images of the cells are shown. Fluorescent intensities range from purple (low) to green (high).

negative 911 cells (result not shown). Confocal laser scanning microscopy was used to analyze the subcellular localization of the pIX_scTCR$^{A1M1}$ protein after virus infection (**Fig. 2c**). Although the majority of the pIX_TCR$^{A1M1}$ protein was observed in the cytoplasm, significant amounts were present in the nuclei of infected cells. In >90% of the infected cells the pIX_TCR$^{A1M1}$ fusion protein was readily detectable in the nucleus.

## Efficient incorporation of pIX_TCR$^{A1M1}$ in the virus capsid

Next, we tested the incorporation of pIX_TCR$^{A1M1}$ into the capsid of the vector HAdV-5.CMVLUCΔE1ΔE3ΔpIX. This vector lacks a functional pIX gene and carries the firefly luciferase reporter gene under control of the cytomegalovirus (CMV) promoter. After transduction of the 911/pIX_TCR$^{A1M1}$ cells with the ΔpIX virus, the offspring virus particles were harvested and purified via the conventional cesium chloride

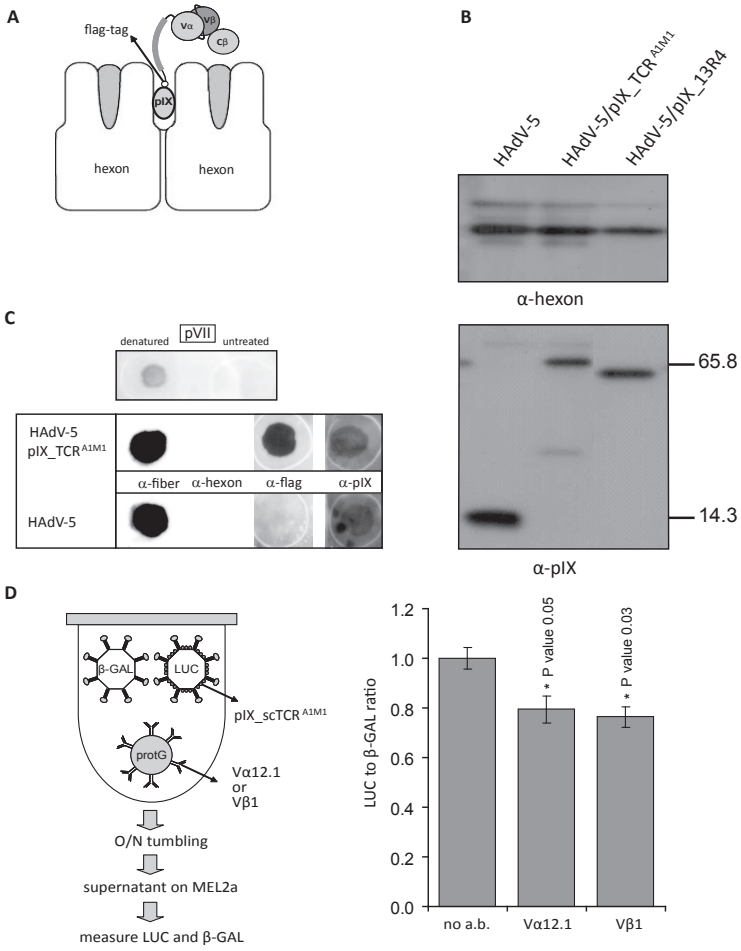


**Figure 3.** Analysis of pIX_TCR$^{A1M1}$ incorporation in the virus capsid. (**a**) Schematic representation of the pIX_TCR$^{A1M1}$ fusion protein exposing the single-chain TCR$^{A1M1}$ above the hexon capsomers. A spacer of 75 Angstrom is included to improve presentation of the single-chain T-cell receptor (scTCR). A flag tag is present in between the C terminus of pIX and the 75-Angstrom spacer. Additional linkers flank the 75-Angstrom spacer (with amino-acid sequence 'ser-gly-gly-gly') to enhance the flexibility of the scTCR. (**b**) Western analysis on virus lysates of cesium chloride (CsCl)-purified viruses to analyze incorporation of pIX_TCR$^{A1M1}$ in the particles. To compare incorporation efficiencies, virus lysates of HAdV-5 and HAdV-5/pIX_13R4 were included. The anti-hexon antibody was included as a virus particle loading control. The predicted size of 14.3 kDa for wild-type pIX and 65.8 kDa for pIX_scTCR$^{A1M1}$ was confirmed by the SDS-PAGE, as indicated in the figure. (**c**) Spot-blot analysis to detect the presence of pIX_TCR$^{A1M1}$ in intact virus particles. Virus was spotted onto a membrane followed by incubation with multiple antibodies. As a control to show integrity of the particles upon the spot-blot treatments, incubation with anti-pVII was included, directed against the core protein VII. Only after denaturation pVII could be detected. (**d**) Binding of pIX_TCR$^{A1M1}$-loaded virus particles on beads containing anti-TCR antibodies (Vα12.1 or Vβ1). After incubation of beads with the pIX_TCR$^{A1M1}$ virus (containing the luciferase reporter as a transgene) plus a control virus (containing the *Escherichia coli* β-galactosidase gene as a transgene), the supernatant was applied to MEL2A cells. The ratio of luciferase to β-galactosidase expression in the cells was subsequently measured, and was normalized to the ratio obtained on mock beads (beads without antibody).

(CsCl) purification method. This resulted in the virus HAdV-5/pIX_TCR$^{A1M1}$. During purification, particle-associated pIX molecules were separated from the nonassociated pIX molecules, as nonassociated variants do not co-purify with the virus particles in the CsCl gradient.[17,33] A schematic representation of the pIX_TCR$^{A1M1}$ fusion protein, with its exposed single-chain TCR$^{A1M1}$ positioned above the hexon capsomers, is depicted in **Fig. 3a**.

The presence of pIX_TCR$^{A1M1}$ in the virus particles was detected by western assay (**Fig. 3b**). The amount of pIX_TCR$^{A1M1}$ in the HAdV-5/pIX_TCR$^{A1M1}$ particles is slightly lower than the amounts of pIX in wild-type (wt) HAdV-5 particles. Loading was similar to the loading of pIX_13R4 in the previously produced virus HAdV-5/pIX_13R4.[18] The 13R4 is a single-chain antibody fragment directed against β-galactosidase, which is approximately 14 kDa smaller than the scTCR$^{A1M1}$.

Incorporation of pIX_TCR$^{A1M1}$ in the virus capsid was also shown by spot-blot analyses (**Fig. 3c**). Virus particles were spotted on a nitrocellulose membrane, followed by incubation with various antibodies. Upon spotting, the virus particles remain intact, indicated by the inability to detect the adenovirus core protein VII (pVII). Only after denaturation of the virus particles the pVII could be detected. From the appearance of the anti-flag signal it can be concluded that flag epitopes of the pIX_TCR$^{A1M1}$ fusion protein were accessible to immunoglobulins in the context of intact virus particles. For the anti-flag and the anti-pIX detection longer exposure times were used, resulting in increased background signals.

To further investigate the accessibility of the single-chain TCR$^{A1M1}$ at the surface of the virus particles we performed an immunoprecipitation assay, in which the ability of the pIX_TCR$^{A1M1}$ virus to bind to anti-TCR antibody-coated beads was analyzed (**Fig. 3d**). The pIX_TCR$^{A1M1}$ virus was mixed with a control virus and subsequently incubated with Vα12.1 or Vβ1 antibody precoated beads. Both antibodies specifically recognize the variable (V) domain of the TCR$^{A1M1}$. After incubation, supernatant fraction, containing virus particles that were not bound to the beads, was applied to MEL2a cells, and the infection ratio of pIX_TCR$^{A1M1}$ virus (containing the luciferase transgene) to control virus (containing the β-galactosidase transgene) was determined. As a result, significantly lower ratio for the Vα12.1- or Vβ1-treated samples was observed when compared to the ratio obtained from the samples without antibody treatment. This shows the binding of intact pIX_TCR$^{A1M1}$ virus particles to the Vα12.1 and Vβ1 antibodies. Thus, it can be concluded that the V domains of the TCR$^{A1M1}$ at the surface of the virus particles are accessible, suggesting that the scTCR may be free to interact with the HLA-A1/MAGE-A1 complex at the cell surface.

## Targeting of the pIXscTCR-containing virus to HLA-A1/MAGE-A1 positive MZ2-MEL3.0 tumor cells

To test the targeting potential of the HAdV-5/pIX_TCR$^{A1M1}$ virus to HLA-A1/MAGE-A1 expressing cells, transduction of MZ2-MEL3.0 melanoma cells (CAR$^{neg}$, HLA-A1$^{pos}$, MAGE-A1$^{pos}$) was analyzed and compared to control virus transduction. The absence of CAR expression is an important aspect to test the targeting potential of the pIX_TCR$^{A1M1}$ containing virus, since the virus is not ablated for its natural CAR-binding ability, which occurs via the fiber attachment protein. In parallel to the infection of MZ2-MEL3.0, the CAR-positive melanoma cell line MEL2a (CAR$^{pos}$, HLA-A1$^{pos}$,

MAGE-A1$^{neg}$) was infected with the viruses to analyze CAR-mediated transduction. Transduction efficiencies of the viruses were determined by measuring luciferase production 24 h after transduction. As represented in **Fig. 4**, presence of the pIX_TCR$^{A1M1}$ fusion protein in the virus capsid results in a highly increased transduction of the target cell line MZ2-MEL3.0. Whereas CAR-mediated transduction on the MEL2a cell line was highest for the pIXscTCR-lacking virus (indicated by a twofold higher luciferase activity), the opposite pattern was obtained for the target cell line MZ2-MEL3.0, which was approximately fourfold better transduced by the pIXscTCR loaded virions. When setting the targeting ratio (MZ2-MEL3.0 / MEL2a) for HAdV-5 at one, the normalized targeting effect for HAdV-5/pIX_TCR$^{A1M1}$ on the MZ2-MEL3.0 cell line is 9.5. The approximate 10-fold increase in transduction specificity on the target cell line did not significantly change by increasing (multiplicity of infection (MOI) = 10,000) or decreasing (MOI = 100) the MOI (results not shown).

## Downmodulation of HLA-A1/MAGE-A1 availability results in decreased targeting by HAdV-5/pIX_TCR$^{A1M1}$

To demonstrate that HAdV-5/pIX_TCR$^{A1M1}$ mediates transduction through binding to HLA molecules at the cell surface, MZ2-MEL3.0 cells were incubated with anti-HLA-ABC antibodies, prior to adding the virus. This resulted in a significant decrease in transduction with the pIXscTCR virus, whereas no decrease was observed for the control virus (**Fig. 5a**). This observation indicates that transduction of the MZ2-MEL3.0 cells is inhibited by the binding of immunoglobulins to HLA molecules.

As an alternative blocking strategy, HLA class I presentation at the surface of MZ2-MEL3.0 was downmodulated by the expression of the human cytomegalovirus (HCMV) US11 protein. The US11 protein causes rapid degradation of newly synthesized HLA class I heavy chains by mediating their retrograde transport or 'dislocation' from the endoplasmic reticulum (ER) into the cytosol, where they are degraded by proteasomes.[34] MZ2-MEL3.0 cells were transduced using retroviruses encoding US11 or a control vector and surface HLA class I levels were analyzed by flow cytometry (**Fig.**

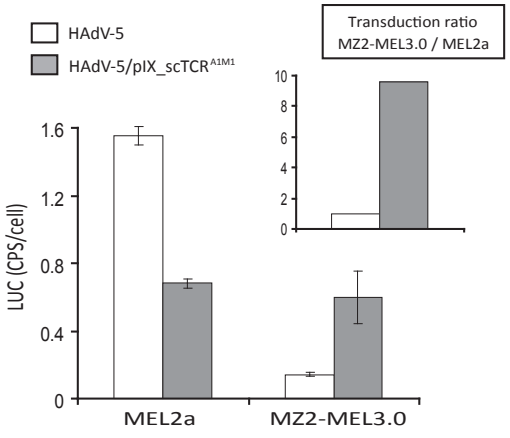


**Figure 4.** Targeting of HAdV-5/pIX_TCR$^{A1M1}$ to HLA-A1/MAGE-A1-presenting MZ2-MEL3.0 cells. The target cell line MZ2-MEL3.0 (HLA-A1$^{pos}$/MAGE-A1$^{pos}$, CAR$^{neg}$) was transduced with HAdV-5 and HAdV-5/pIX_TCR$^{A1M1}$. In parallel, transduction of the MEL2a cell line was performed to determine fiber-CAR-mediated transduction of both vectors. As transduction readout, luciferase production was determined 24 h after transduction. Multiplicity of infection was 1000 virus particles per cell. The insert graph shows the ratio of MZ2-MEL3.0 to MEL2a transduction for the targeted virus HAdV-5/pIX_TCR$^{A1M1}$, which is normalized to the ratio for the control virus. The presence of pIX_TCR$^{A1M1}$ results in a 10-fold improved transduction of the MZ2-MEL3.0 cell line.

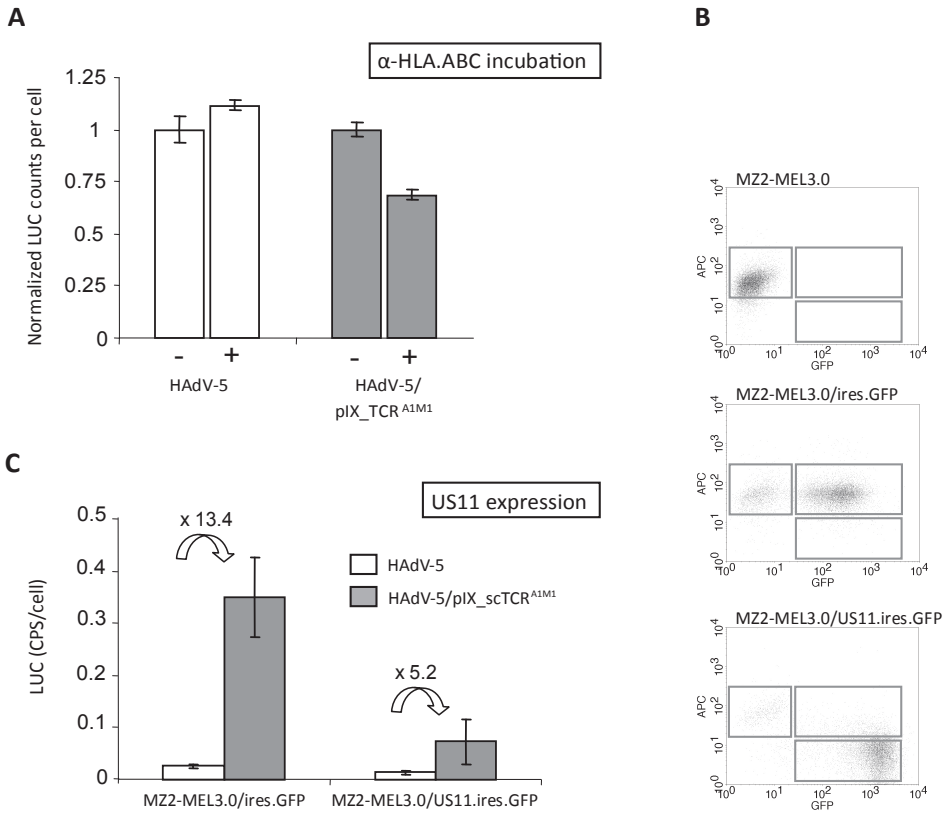


**Figure 5.** Downmodulation of human leukocyte antigen (HLA) availability results in decreased targeting. (**a**) Incubation of MZ2-MEL3.0 with anti-HLA-ABC antibody results in a significant decrease in HAdV-5/pIX_TCR$^{A1M1}$ transduction. Transduction of the control virus is not downregulated after anti-HLA-ABC loading. (**b**) Flowcytometric analysis shows downregulation of HLA class I presentation at the cell surface of MZ2-MEL3.0 cells after infection with the retroviral vector pLZRS.US11.ires.GFP or the control vector pLZRS.ires.GFP. The dot plots show for both transductions the presence of green fluorescent protein (GFP)-positive cells (shift to the right). The downshift in case of the pLZRS.US11.ires.GFP transduction indicates the downregulation of HLA class I presentation (detection via B9.12.1 antibody plus allophycocyanin (APC)-conjugated secondary antibody). (**c**) Decrease in HAdV-5/pIX_TCR$^{A1M1}$ targeting after US11-mediated downregulation of HLA class I molecules. Compared to the control cell line, the ratio HAdV-5/pIX_TCR$^{A1M1}$ to HAdV-5 transduction is lower for the US11-expressing cell line (ratios of respectively 13.2 and 5.2). Multiplicity of infection was 1000 virus particles per cell. Luciferase production was measured 24 h after transduction.

**5b**). The MZ2-MEL3.0 cells were efficiently transduced with the retroviruses, since the majority of the cells was positive for the vector-mediated green fluorescent protein (GFP) expression. The downshift of the US11-expressing cells in the dotplots indicates the downregulation of HLA class I presentation. Next, luciferase production after HAdV-5/pIX_TCR$^{A1M1}$ and HAdV-5 transduction was measured in the cell lines MZ2-MEL3.0/US11.ires.GFP and MZ2-MEL3.0/ires.GFP (**Fig. 5c**). This revealed a decrease in pIX_TCR$^{A1M1}$ mediated targeting for the US11 expressing cells. Complete blocking

of targeting did not occur, probably as a result of incomplete downregulation of HLA class I expression.

## Further analysis on different cell lines to confirm specificity of targeting to HLA-A1/MAGE-A1

During the time course of our study, the cell line MZ2-MEL43 became available. This line is CAR$^{neg}$, HLA-A1$^{pos}$, and MAGE-A1$^{pos}$. Since the level of HLA-A1 expression

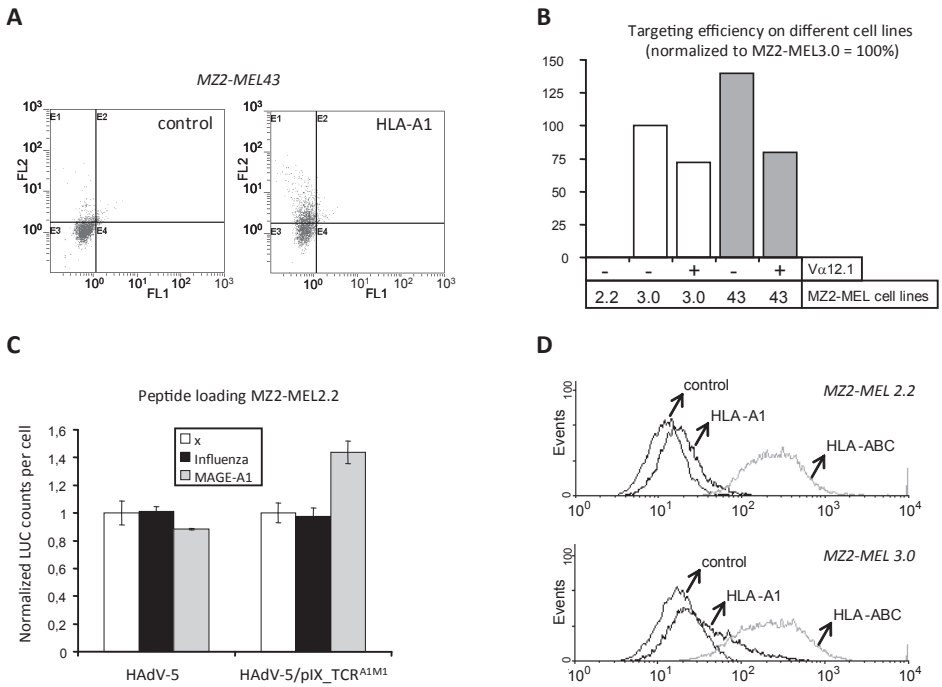


**Figure 6.** Comparison of the targeting on multiple cell lines to further confirm HLA-A1/MAGE-A1 specificity. (**a**) Flow cytometry analysis of human leukocyte antigen (HLA)-A1 expression at the surface of MZ2-MEL43 cells. The control plot represents incubation with secondary antibody only. (**b**) The targeting efficiency of the HAdV-5/pIX_TCR$^{A1M1}$ virus on three different cell lines was determined, and normalized to the targeting on MZ2-MEL3.0 cells equal to 100%. Enhanced transduction of the pIXscTCR virus compared to the control virus was observed for the cell line MZ2-MEL43. This cell line was more efficiently targeted than the MZ2-MEL3.0 cells. No specific targeting was obtained on the melanoma-associated antigen (MAGE)-A1-negative cell line MZ2-MEL2.2. A decrease in targeting was obtained after incubation of the pIXscTCR virus with Vα12.1 antibody. (**c**) Improved transduction of MZ2-MEL2.2 cells after loading with MAGE-A1 peptide. MAGE-A1 peptide or an irrelevant peptide derived from influenza virus A nucleoprotein antigen was added to the wells 2 h before transduction with HAdV-5/pIX_TCR$^{A1M1}$. Luciferase production was measured 24 h after transduction and was normalized to transduction on nonpeptide-loaded cells. (**d**) Flow cytometry analysis to compare the presentation of HLA-A1 and HLA-ABC at the cell surface of MZ2-MEL2.2 and MZ2-MEL3.0 cells. The control graphs represent incubation with secondary antibody only. The MZ2-MEL3.0 cell line had significantly more anti-HLA-A1 events in the higher phycoerythrin (PE) range, indicating a higher number of HLA-A1 molecules per cell.

appeared to be at least equal to the HLA-A1 level of the target cell line MZ2-MEL3.0 (**Fig. 6a**), the targeting efficiency of HAdV-5/pIX_TCR$^{A1M1}$ to MZ2-MEL43 and MZ2-MEL3.0 was analyzed in parallel (**Fig. 6b**). A third cell line, MZ2-MEL2.2, which is a derivative from MZ2-MEL3.0 but does not express MAGE-A1, was included as well. As expected, transduction with the pIXscTCR virus was enhanced in cell line MZ2-MEL43. Interestingly, the targeting efficiency was 45% higher to MZ2-MEL43 than to MZ2_MEL3.0. As expected, no targeting was obtained on the MAGE-A1-negative cell line MZ2-MEL2.2, demonstrating the absolute requirement for MAGE-A1 presentation. The enhanced transduction in the two HLA-A1/MAGE-A1-positive cell lines was blocked by incubation of the pIXscTCR virus with the antibody Vα12.1 (**Fig. 6b**), confirming that the targeting is dependent on the scTCR in the capsid.

To further analyze the specificity of targeting, MZ2-MEL2.2 cells (CAR$^{neg}$, HLA-A1$^{pos}$, MAGE-A1$^{neg}$) were loaded either with a control peptide (an irrelevant peptide derived from influenza virus A nucleoprotein), a MAGE-A1 peptide, or were mock treated, and were subsequently exposed to the pIXscTCR virus (**Fig. 6c**). Incubation of the cells with MAGE-A1 peptide, but not with the control peptide, resulted in a significant increase in transduction by HAdV-5/pIX_TCR$^{A1M1}$. This effect did not occur in HAdV-5 transduction, confirming the dependency of HAdV-5/pIX_TCR$^{A1M1}$ transduction on the presentation of the MAGE-A1 on HLA-A1. Compared to the MZ2-MEL3.0 cell line, the targeting efficiency to MAGE-A1-loaded MZ2-MEL2.2 cells was rather low. This can be explained by the significantly lower number of HLA-A1 molecules at the cell surface (**Fig. 6d**).

## DISCUSSION

We demonstrate successful targeting of HAdV-5 vectors to HLA-A1/MAGE-A1-presenting tumor cells using an scTCR incorporated in the capsid as a genetic fusion with pIX. The pIX_TCR$^{A1M1}$-loaded virions transduced HLA-A1/MAGE-A1-expressing cells and HLA-A1-expressing cells loaded with MAGE-A1 peptides. These findings warrant further exploration of minor capsid pIX as an anchor for the insertion of targeting moieties.

The fusion of targeting proteins to pIX has some potential advantages. The use of pIX allows the incorporation of larger numbers of targeting molecules since it is present in 240 copies whereas 36 fiber molecules are present per virion. Furthermore, incorporation of large targeting ligands in the fiber, such as scTCRs or scFv's, may lead to a reduced number of fiber molecules per virion.[35] Intriguingly, pIX fusion proteins with sizes of up to 120 kDa can be accommodated in the capsid, although incorporation efficiency of the modified pIX (linked to an HSV1-TK/luciferase fusion protein) was slightly decreased.[36] However, this may be improved by the use of α-helical spacers.[17]

To produce our targeting virus, with pIX_TCR$^{A1M1}$ incorporated in the capsid, we used pIX-producing helper cell lines generated via lentiviral transduction.[37] By using this strategy of incorporation of pIX in a ΔpIX virus, the time-consuming process of making viruses with pIX modifications in the genome can be avoided. Efficient incorporation of modified pIX, for example, linked to single-chain antibody fragments, can be obtained.[18] After transduction of 911 helper cells that produce the pIX_TCR$^{A1M1}$ protein, production of pIX_TCR$^{A1M1}$ in the cells was verified by immunohistochemistry.

Infection of the transduced helper cells with ΔpIX virus resulted in the production of virus particles with close to wt level of the pIX_TCR$^{A1M1}$ protein incorporated in their capsid, demonstrating the usefulness of this approach.

Interestingly, pIX_TCR$^{A1M1}$ was detected predominantly in the cytoplasm of the LV.pIX_TCR$^{A1M1}$-transduced 911 helper cells. This is in contrast to the location of the wt pIX, which is mainly nuclear.[38] As can be concluded from our results, the aberrant subcellular localization of pIX_TCR$^{A1M1}$ does not hamper incorporation in the virus capsid. Since adenovirus particles are assembled in the nucleus, these results imply that a sufficient amount of pIX_TCR$^{A1M1}$ was present in the nuclei during formation of the HAdV-5/pIX_TCR$^{A1M1}$ virus. Indeed, we could confirm by confocal microscopy that during the adenovirus infection significant amounts of pIX_TCR$^{A1M1}$ are localized in the nucleus.

The targeting specificity to tumor cells expressing the MAGE-A1-derived epitope in the context of HLA-A1 was demonstrated via different approaches. First, transduction of the HLA-A1/MAGE-A1-positive MZ2-MEL3.0 cells was increased up to 10-fold by the incorporation of pIX_TCR$^{A1M1}$ in the virus capsid. The targeting efficiency in another HLA-A1/MAGE-A1-positive cell line, MZ2-MEL43, appeared to be higher. Specificity was also evident from experiments in which HLA-A1-positive/MAGE-A1-negative MZ2-MEL2.2 cells were loaded with MAGE-A1 peptides. This resulted in a significant increase in transduction efficiency. The targeting specificity was lower than achieved on MZ2-MEL3.0 cells. This may be due to distinct presentation of synthetic peptides when compared to endogenously processed and presented peptides at the cell surface. Also, MZ2-MEL2.2 cells express fewer HLA-A1 molecules at their cell surface than MZ2-MEL3.0 cells (**Fig. 6d**). Furthermore, the targeting efficiency to MZ2-MEL3.0 could be reduced by blocking HLA, either via incubation of the cells with anti-HLA-ABC antibody, or alternatively, via the expression of the HCMV US11 gene. The US11 causes degradation of newly synthesized MHC class I heavy chains by mediating their dislocation from the ER into the cytosol.[34] For the antibody incubation, as well as the US11-mediated downregulation, the blocking of targeting was not 100%. Apparently, the incubation of cells with anti-HLA-ABC antibody was not sufficient to block all HLA-A1 molecules. In case of the US11-mediated downmodulation, flow cytometry analysis showed that a small but detectable fraction of the cell population had not been transduced (GFP negative), and thus did not downregulate HLA class I presentation, which probably explains the incomplete block of targeting.

We report successful targeting of HAdV-5 via fusion of a specific targeting moiety to capsid pIX. It has been speculated that targeting via pIX results in entrapment of the virions in the endosomes, caused by high-affinity interaction between the pIX fusion protein and the cellular receptor.[16] However, binding of T-cell receptors to their target MHCI/peptide complex is known to have low affinity.[39] This may allow the scTCR-containing virions to escape from the endosome. Alternatively, binding of the virus particles to the HLA-A1/MAGE-A1 complex may have resulted in a distinct internalization, that is, differing from the normal HAdV-5 internalization via clathrin-coated vesicles. Cellular internalization mediated by binding to MHCI molecules is exploited by Simian virus 40, which enters the cell via a unique pathway that involves caveolae, rather than clathrin-coated pits.[40] Interestingly, HLA class I has been suggested as an alternative receptor for HAdV-5.[41]

The fact that the scTCR used in this study is biologically active at the surface of the adenovirus supports the feasibility of targeting adenovirus vectors by fusing complex polypeptide molecules, such as scTCRs or scFv fragments, to capsid pIX. Normally, such complex polypeptides are routed via the protein secretory pathway. This aspect might hamper functional incorporation in the capsid of adenovirus particles, which are assembled in the nucleus. The reducing environment in the cell prevents the formation of disulfide bridges, which may result in improper folding of these proteins.[42] Another obstacle for the implementation of scTCRs in adenoviral vectors might be that the relatively large scTCRs hamper correct virion formation or might interfere with crucial processes necessary for virus propagation. Initial attempts to produce adenovirus vectors with an scTCR fragment genetically fused to a knobless fiber protein were unsuccessful.[43] Incorrect folding and/or trimer formation of the fiber protein due to the presence of the scTCR fragment was reported to be the most likely explanation. The incorrect fiber formation might have caused the inability to rescue the virus, even though the mutated viral DNA was introduced into the target cell line. However, more recently the successful development of an scTCR-containing adenovirus has been reported.[6] Our results, with an scTCR bound to the minor capsid pIX, emphasize the potential of scTCRs for obtaining transductional specificity in adenoviral vectors. The pIX_TCR$^{A1M1}$ fusion protein was incorporated in the capsid with high efficiency. Although it remains to be established whether all scTCRs are functional if fused with pIX, our results clearly demonstrate the functionality of at least part of the scTCRs. The variable domains of the scTCR, which mediate binding to the HLA-A1/MAGE-A1 target complex, were accessible to antibodies in the context of intact virions, which was shown via immunoprecipitation of the virus on Vα12.1- or Vβ1-coated beads, and alternatively, via downregulation of transduction as a result of Vα12.1 incubation. The presence of the 75-Angstrom α-helical spacer[17] in between the scTCR and pIX domains might have been crucial to generate sufficient flexibility for proper orientation of the scTCR at the capsid surface. Detailed studies on elucidating the process of scTCR folding during virus infection would be of great interest. Our immunohistochemistry analysis on the 911/pIX_TCR$^{A1M1}$ cell line yielded staining with the conformation-dependent antibody Vα12.1, only after adenovirus infection. It is tempting to speculate that the scTCR only adopts its proper conformation upon change of the intracellular milieu upon induction of adenovirus-induced cell death.

The pIXscTCR-containing virus used in this study was not de-targeted, as the CAR-binding elements, the heparan sulfate proteoglycans-binding elements and the plasma protein-binding elements are still present in the capsid. For the final aim of *in vivo* tumor therapy via delivery of an HAdV-5 vector, these elements should be abolished. Also, it would be interesting to test whether shortening of the fiber shaft or complete removal of the fiber improves targeting efficiency, for instance by reducing steric hindrance of the pIXscTCR molecules by the protruding fiber proteins. Currently, pIXscTCR targeting in the context of fiber mutations is under investigation.

Our approach as described here utilizes the targeting of CT antigen epitopes that are presented at the cell surface of tumor cells by HLA class I molecules. This principle differs from previously reported retargeting approaches of adenovirus-based vectors, which encompass the targeting of 'overexpression' receptors like Her2/neu[44] or the epidermal growth factor receptor.[45] The expression profile of the CT antigens

is generally much more specific compared to the expression profile of the 'more conventional' target molecules such as the overexpressed receptors. The fact that HLA class I/CT antigen complexes can elicit a highly specific response of the immune system has prompted many studies on immune cell modifications with the aim to direct the modified cells toward tumor cells.[4] However, tumor therapies via such approaches may not be feasible since the process of isolating, modifying and expansion of patient immune cells is likely to be difficult and time consuming. Viral vector-based cancer gene therapy might be a more suitable strategy. Genetic modification of adenoviral vectors, which are the most widely used virus vectors in clinical tumor gene therapy studies, is relatively easy. Besides, adenoviruses have a good safety profile and can be produced with high titers.

Our results show that HAdV-5 vectors can be genetically modified to mediate greatly enhanced gene delivery into tumor cells by targeting HLA class I/CT antigen complexes. The successful combination of two aspects with great potential in cancer gene therapy, adenovirus as a vector and CT antigens as a target, clearly warrants further exploration. Follow-up studies are under way, and especially the fusion of other scTCRs to pIX (directed against other HLA class I/CT antigen complexes), and the evaluation of *in vivo* performance of the modified HAdV-5 vectors will be of great interest.



# METHODS

## DNA constructs

The lentiviral vectors used in this study were described in earlier studies.[37] Plasmid pLV.CMV.pIXflag75AscTCR$^{A1M1}$.bc.neo, abbreviated as pLV.pIX_TCR$^{A1M1}$, was constructed by standard cloning procedures. The pLV plasmid contained a G418 resistance gene (neo) downstream of the pIX_TCR$^{A1M1}$ sequence, separated by an internal ribosome entry site (bc). In between the pIX and scTCR sequence, sequences are present that encode a flag tag and a 75-Angstrom spacer. Insertion of this spacer has been shown to greatly enhance presentation of pIX-fused proteins at the virus capsid.[17] The gene for pIXflag75 was obtained from the pcDNA3.1-based construct pAd5pIXflag75MYC.[17] The gene encoding scTCR$^{A1M1}$ was subcloned from the retroviral vector pBullet.VαVβCβ.[46] The scTCR$^{A1M1}$ sequence of pBullet.VαVβCβ was originally constructed from the Vα, Vβ and Cβ sequences from an HLA-A1/MAGE-A1-specific CTL clone MZ2-82/30 of patient MZ2.[47]

## Cells

All cell lines were maintained at 37 °C in a humidified atmosphere of 5% $CO_2$ in Dulbecco's modified Eagle's medium (DMEM, Gibco-BRL, Breda, the Netherlands) supplemented with 8% fetal bovine serum (FBS, Gibco-BRL) and penicillin-streptomycin mixture. Cell lines used for the adenovirus targeting experiments were the melanoma cell lines MEL2a, MZ2-MEL2.2, MZ2-MEL3.0 and MZ2-MEL43. Expression status of the CAR and HLA-A1/MAGE-A1 has been described before for the cell lines MEL2a (CAR$^{pos}$/HLA-A1$^{pos}$/MAGE-A1$^{neg}$), MZ2-MEL2.2 (CAR$^{neg}$/HLA-A1$^{pos}$/MAGE-A1$^{neg}$) and MZ2-MEL3.0 (CAR$^{neg}$/HLA-A1$^{pos}$/MAGE-A1$^{pos}$).[6] The status of the previously uncharacterized cell line MZ2-MEL43 is CAR$^{neg}$/HLA-A1$^{pos}$/MAGE-A1$^{pos}$, as determined by flow cytometry

analysis and shown in **Fig. 6a** in this paper. The HAdV-5 E1-transformed cell line 911 was used to propagate and titer adenovirus vectors.[48]

## Lentiviral and retroviral transductions

The recombinant lentivirus LV.pIX_TCR$^{A1M1}$ was produced as described elsewhere.[37] The lentivirus titer was determined by p24 enzyme-linked immunosorbent assay, assuming that 1 ng p24 equals $2.5 \times 10^3$ transducing units.[49] To establish a helper cell line stably expressing pIX_TCR$^{A1M1}$, 911 cells were transduced with the recombinant lentivirus, resulting in the cell line 911/pIX_TCR$^{A1M1}$. Infection was done with five transducing units per cell. To select for stably transduced cells, the cell line 911/pIX_TCR$^{A1M1}$ was cultured in medium supplemented with 200 mg $l^{-1}$ G418 (Invitrogen, Breda, the Netherlands).

The retroviral vector pLZRS-US11-IRES-EGFP was made by subcloning the HCMV US11 cDNA fragment into the pLZRS-IRES-EGFP vector.[50] This construct was used, together with the wt enhanced green fluorescent protein (EGFP)-expressing retroviral vector, to produce amphotropic retrovirus by transfection of the Phoenix cell line with the calcium phosphate method (www.stanford.edu/group/nolan/retroviral_systems/retsys.html). Transfected cells were grown under puromycin selection (2 µg $ml^{-1}$), which was removed 24 h before collecting the virus. MZ2-MEL3.0 cells, grown on retronectin-coated dishes (Takara, Japan), were transduced with the recombinant viruses to create cells stably expressing US11 and the control construct.

## Adenovirus vectors

The 911/pIX_TCR$^{A1M1}$ helper cell line was transduced with the replication-deficient adenoviral vector HAdV-5.CMVLUCΔE1ΔE3ΔpIX. Production and characteristics of this vector are described elsewhere.[17] The vector carries a firefly luciferase transgene under control of the human CMV immediate-early promoter. In this vector the pIX gene had been deleted from the genome. Three days after transduction, the offspring virus was harvested and purified by CsCl banding, resulting in the virus HAdV-5.CMVLUCΔE1ΔE3ΔpIX+pIX_TCR$^{A1M1}$ (indicated in this paper as HAdV-5/pIX_TCR$^{A1M1}$). Adenovirus particle titers were determined by measuring optical density at 260 nm, using a standard protocol.[51] The control virus used in all retargeting experiments was HAdV-5.CMVLUCΔE1ΔE3 (indicated as HAdV-5).

## Immunohistochemistry

Immunohistochemistry was performed on the helper cell line 911/pIX_TCR$^{A1M1}$, with or without HAdV-5.CMVLUCΔE1ΔE3ΔpIX infection. Infection was performed with 1000 virus particles per cell, 24 h before fixation. After washing with phosphate-buffered saline (PBS), the cells were fixed in acetone/methanol (1:1) for 10 min at room temperature. Staining was performed with the antibodies anti-pIX (rabbit polyclonal (1:500), kindly provided by Dr Keith Leppard, University of Warwick, UK),[52] Vα12.1 (Pierce-Endogen Biotechnology, Rockford, IL, USA) and anti-hexon (clone BOD604, fluorescein isothiocyanate (FITC)-conjugated, Biodesign International, Saco, ME, USA). FITC-labeled antibodies (Jackson ImmunoResearch, France) were used as secondary antibody. Upon analysis of the uninfected cells, the nuclei were stained using propidium iodide. The exact detection procedure has been described previously.[18]

Wide-field microscopy was performed with a Leica DM-IRBE microscope. Confocal laser scanning microscopy was performed on a confocal microscope system (model TCS/SP2; Leica). Z-series images (slice spacing 0.45 µm) were acquired with a 63_ NA 1.4 plan Apo objective and were analyzed with Leica confocal software.

## Immunoblotting procedures

Western analysis was performed to analyze production of pIX_TCR$^{A1M1}$ in the helper cells and to analyze incorporation efficiency of pIX_TCR$^{A1M1}$ in the virus capsid. Cell lysates were made in radioimmunoprecipitation assay lysis buffer (50 mM Tris (pH 7.5), 150 mM NaCl, 0.1% SDS, 0.5% DOC, 1% NP40). Protein concentrations were measured with the bicinchoninic acid protein assay (Pierce Biotechnology, Perbio Science BV, Etten-Leur, the Netherlands). Virus lysates were prepared by adding 5 × $10^9$ virus particles directly to western sample buffer. The pIX variants were visualized with rabbit polyclonal anti-pIX serum (1:2000).[52] Goat polyclonal anti-hexon (1:1000) (Abcam, Cambridge, UK) was used as a virus particle loading control. Secondary antibodies were horseradish peroxidase (HRP)-conjugated goat-anti-rabbit and rabbit-anti-mouse (Santa Cruz Biotechnology, Inc., Santa Cruz, CA, USA). The western blotting and detection procedures have been previously described.[17, 37]

A spot-blot type analysis was used to detect viral capsid proteins in intact virus particles. Immobilon membrane (Millipore, Etten-Leur, The Netherlands) was activated with methanol, washed for 10 min with PBS and virus (3 × $10^9$ particles) was spotted onto the membrane. Virus was spotted as intact particles (untreated) or as virus lysate (denatured through adding western sample buffer plus 5 min incubation at 98 °C). This was followed up by blocking for 1 h in Soja milk (Alpro soja, Breda, The Netherlands), and washing twice for 10 min with 0.2% Tween 20 in PBS. Thereafter, probing of capsid proteins was performed according to the same protocol as applied for the western analysis. The primary antibodies used were mouse monoclonal anti-fiber knob (1D6.14, 1:1000),[53] goat polyclonal anti-hexon (1:2000; Abcam), anti-flag (1:500) (anti-flag M2 Affinity Gel Freezer-Safe; Sigma-Aldrich Chemie, Zwijndrecht, the Netherlands), rabbit polyclonal anti-pIX (1:2000)[52] and anti-pVII antibody (1:500) (kindly provided by Saw See Hong, Laboratoire de Virologie et Pathogénèse Virale, Lyon, France). Secondary antibodies used were HRP-conjugated goat-anti-rabbit and rabbit-anti-mouse (Santa Cruz Biotechnology).

## Binding of virus particles to anti-TCR coated beads

The ability of the pIX_TCR$^{A1M1}$ virus to bind to anti-TCR-coated beads was investigated through an immunoprecipitation assay. Protein G Sepharose beads (30 µl; Pierce Biotechnology) were incubated with 1 µg of antibody (Vα12.1 or Vβ1), for 2 h at 4 °C in 600 µl cold PBS. Antibody-coupled beads were added to 1 ml DMEM without serum, containing two types of virus; HAdV-5.CMVLUCΔE1ΔE3ΔpIX (5 × $10^{10}$ particles), and HAdV-5.CMVLacZΔE1 (5 × $10^{10}$ particles). Control samples were incubated with beads only. After incubation for 12 h at 4 °C, 50 µl of the supernatant was added to 450 µl DMEM (containing 8% FBS), which was subsequently applied on MEL2a cells in a 24-well plate. After 24 h, the expression levels of intracellular luciferase and β-galactosidase were determined. To this end, the cells were washed once with PBS, and lysed in 100 µl LUC-lysis mix (25 mM Tris-phosphate (pH 7.8), 2 mM CDTA,

2 mM DTT, 10% glycerol and 1% Triton-X in PBS). After shaking for 15 min at room temperature, lysates were centrifuged (10000 *g*, 10 min). Luciferase production was determined with Promega Luciferase Assay, and β-galactosidase production was determined with the Tropix Galacto-Light reporter gene assay (Applied Biosystems, Bedford, MA, USA). Light intensity measurement was performed in a Victor Wallac 2 microplate reader (PerkinElmer, Inc., Waltham, MA, USA).

### Virus transduction assays

Transduction efficiencies with HAdV-5/pIX_TCR$^{A1M1}$ and HAdV-5 were analyzed by measuring luciferase production. For all virus transduction assays, transduction was performed in a 24-well plate, with 1000 viral particles per cell, in 500 µl DMEM/8% FBS. After 24 h, luciferase production was measured as described above (25 µl luciferase assay reagent was added to 10 µl lysate).

Incubation of cells with anti-HLA-ABC antibody (ascites) was performed to test downmodulation of targeting. The cells were incubated for 12 h with 20 µg ml$^{-1}$ anti-HLA-ABC (in medium), which was removed from the cells before adding the virus. TCR blocking analysis was performed by incubating the virus ($10^8$ particles) for 12 h (4 °C) with 150 ng Vα12.1 antibody in 100 µl PBS supplemented with 2% horse serum. After adding 400 µl medium, the virus was added to $10^5$ cells (resulting in a titer of 1000 particles per cell).

For peptide loading of the MZ2-MEL2.2 cells, 500 ng MAGE-A1 peptide, or 500 ng of an irrelevant peptide derived from influenza virus A nucleoprotein antigen[54] was added per well 2 h prior to adding the virus.

### Flow cytometry

To perform flow cytometry analysis on the different cell lines, the cells were trypsinized, resuspended in PBS (containing 0.5% bovine serum albumin and 0.02% sodium azide), and were incubated with antibodies. The cells were incubated with saturating conditions of anti-CAR antibody,[55] anti-HLA-ABC antibody (W6/32, Cedarlane, ON, Canada) or anti-HLA-A1 antibody (One Lambda, CA, USA) for 30 min on ice, followed by incubation with phycoerythrin (PE)-labeled secondary antibody (Caltac Laboratories, Burlingame, CA, USA) for 30 min on ice. The status of HLA-ABCGE expression at the cell surface of the US11-expressing MZ2-MEL3.0 cell line and the control lines was performed by using anti-HLA-ABCGE (B9.12.1, Immunotech, Marseille, France) as primary antibody and allophycocyanin (APC)-conjugated goat-anti-mouse immunoglobulin G (Jackson ImmunoResearch) as secondary antibody. Flow cytometry data were analyzed with CellQuest software (Becton Dickinson).

## ACKNOWLEDGEMENTS

We thank Karien Wiesmeijer (Molecular Cell Biology, LUMC, Leiden) for performing the confocal microscopy, and Saw See Hong (Laboratoire de Virologie et Pathogénèse Virale, Lyon, France) for providing us with the anti-pVII antibody. This work was supported by the European Union through the 6th Framework Program GIANT (contract no. 512087).

## REFERENCES


1. Van den Eynde BJ, Mandruzzato S, Gueguen M, van der Bruggen P, Marchand M, Coulie PG, *et al.* Tumor antigens recognized by cytolytic T lymphocytes. *Cancer Gene Ther* 1997; **4**: 308.
2. Scanlan MJ, Simpson AJ, Old LJ. The cancer/testis genes: review, standardization, and commentary. *Cancer Immun* 2004; **4**: 1.
3. Yang B, O'Herrin SM, Wu J, Reagan-Shaw S, Ma Y, Bhat KMR, et al. MAGE-A, mMage-b, and MAGE-C proteins form complexes with KAP1 and suppress p53-dependent apoptosis in MAGE-positive cell lines. *Cancer Res* 2007; **67**: 9954-9962.
4. Willemsen RA, Debets R, Chames P, Bolhuis RLH. Genetic engineering of T cell specificity for immunotherapy of cancer. *Hum Immunol* 2003; **64**: 56-68.
5. Peng KW, Holler PD, Orr BA, Kranz DM, Russell SJ. Targeting virus entry and membrane fusion through specific peptide/MHC complexes using a high-affinity T-cell receptor. *Gene Ther* 2004; **11**: 1234-1239.
6. Sebestyen Z, de Vrij J, Magnusson M, Debets R, Willemsen R. An oncolytic adenovirus redirected with a tumor-specific T-Cell receptor. *Cancer Res* 2007; **67**: 11309-11316.
7. Glasgow JN, Everts M, Curiel DT. Transductional targeting of adenovirus vectors for gene therapy. *Cancer Gene Ther* 2006; **13**: 830-844.
8. Wickham TJ, Mathias P, Cheresh DA, Nemerow GR. Integrin-alpha-V-beta-3 and integrin-alpha-V-beta-5 promote adenovirus internalization but not virus attachment. *Cell* 1993; **73**: 309-319.
9. Cohen CJ, Shieh JT, Pickles RJ, Okegawa T, Hsieh JT, Bergelson JM. The coxsackievirus and adenovirus receptor is a transmembrane component of the tight junction. *Proc Natl Acad Sci U S A* 2001; **98**: 15191-15196.
10. Vigne E, Mahfouz I, Dedieu JF, Brie A, Perricaudet M, Yeh P. RGD inclusion in the hexon monomer provides adenovirus type 5-based vectors with a fiber knob-independent pathway for infection. *J Virol* 1999; **73**: 5156-5161.
11. Wu HJ, Han T, Belousova N, Krasnykh V, Kashentseva E, Dmitriev I, *et al.* Identification of sites in adenovirus hexon for foreign peptide incorporation. *J Virol* 2005; **79**: 3382-3390.
12. Einfeld DA, Brough DE, Roelvink PW, Kovesdi I, Wickham TJ. Construction of a pseudoreceptor that mediates transduction by adenoviruses expressing a ligand in fiber or penton base. *J Virol* 1999; **73**: 9130-9136.
13. Dmitriev IP, Kashentseva EA, Curiel DT. Engineering of adenovirus vectors containing heterologous peptide sequences in the C terminus of capsid protein IX. *J Virol* 2002; **76**: 6893-6899.
14. Le LP, Everts M, Dmitriev IP, Davydova JG, Yamamoto M, Curiel DT. Fluorescently labeled adenovirus with pIX-EGFP for vector detection. *Mol Imaging* 2004; **3**: 105-116.
15. Meulenbroek RA, Sargent KL, Lunde J, Jasmin BJ, Parks RJ. Use of adenovirus protein IX (pIX) to display large polypeptides on the virion-generation of fluorescent virus through the incorporation of pIX-GFP. *Mol Ther* 2004; **9**: 617-624.
16. Campos SK, Parrott MB, Barry MA. Avidin-based targeting and purification of a protein IX-modified, metabolically biotinylated adenoviral vector. *Mol Ther* 2004; **9**: 942-954.
17. Vellinga J, Rabelink MJWE, Cramer SJ, van den Wollenberg DJM, Van der Meulen H, Leppard KN, *et al.* Spacers increase the accessibility of peptide ligands linked to the carboxyl terminus of adenovirus minor capsid protein IX. *J Virol* 2004; **78**: 1-10.
18. Vellinga J, de Vrij J, Myhre S, Uil T, Martineau P, Lindholm L, *et al.* Efficient incorporation of a functional hyper-stable single-chain antibody fragment protein-IX fusion in the adenovirus capsid. *Gene Ther* 2007; **14**: 664-670.
19. Glasgow JN, Kashentseva E, Dmitriev IP, Curiel DT. Adenovirus polypeptide IIIa as a novel locale for incorporation of heterologous peptides. *Mol Ther* 2005; **11**: S338.
20. Vellinga J, Van der Heijdt S, Hoeben RC. The adenovirus capsid: major progress

in minor proteins. *J Gen Virol* 2005; **86**: 1581-1588.

21. Furcinitti PS, Van Oostrum J, Burnett RM. Adenovirus polypeptide-IX revealed as capsid cement by difference images from electron-microscopy and crystallography. *EMBO J* 1989; **8**: 3563-3570.
22. Van Oostrum J, Burnett RM. Molecular composition of the Adenovirus type-2 virion. *J Virol* 1985; **56**: 439-448.
23. Saban SD, Nepomuceno RR, Gritton LD, Nemerow GR, Stewart PL. CryoEM structure at 9 angstrom resolution of an adenovirus vector targeted to hematopoietic cells. *J Mol Biol* 2005; **349**: 526-537.
24. Marsh MP, Campos SK, Baker ML, Chen CY, Chiu W, Barry MA. Cryoelectron microscopy of protein IX-modified adenoviruses suggests a new position for the C terminus of protein IX. *J Virol* 2006; **80**: 11881-11886.
25. Fabry CMS, Rosa-Calatrava M, Conway JF, Zubieta C, Cusack S, Ruigrok RWH, *et al.* A quasi-atomic model of human adenovirus type 5 capsid. *EMBO J* 2005; **24**: 1645-1654.
26. Saban SD, Silvestry M, Nemerow GR, Stewart PL. Visualization of alpha-helices in a 6-angstrom resolution cryoelectron microscopy structure of adenovirus allows refinement of capsid protein assignments. *J Virol* 2006; **80**: 12049-12059.
27. Zufferey R, Dull T, Mandel RJ, Bukovsky A, Quiroz D, Naldini L, *et al.* Self-inactivating lentivirus vector for safe and efficient *in vivo* gene delivery. *J Virol* 1998; **72**: 9873-9880.
28. Mautino MR, Ramsey WJ, Reiser J, Morgan RA. Modified human immunodeficiency virus-based lentiviral vectors display decreased sensitivity to trans-dominant rev. *Hum Gene Ther* 2000; **11**: 895-908.
29. Barry SC, Harder B, Brzezinski M, Flint LY, Seppen J, Osborne WRA. Lentivirus vectors encoding both central polypurine tract and posttranscriptional regulatory element provide enhanced transduction and transgene expression. *Hum Gene Ther* 2001; **12**: 1103-1108.
30. Sirven A, Pflumio F, Zennou V, Titeux M, Vainchenker W, Coulombel L, *et al.* The human immunodeficiency virus type-1 central DNA flap is a crucial determinant for lentiviral vector nuclear import and gene transduction of human hematopoietic stem cells. *Blood* 2000; **96**: 4103-4110.
31. Follenzi A, Ailles LE, Bakovic S, Geuna M, Naldini L. Gene transfer by lentiviral vectors is limited by nuclear translocation and rescued by HIV-1 pol sequences. *Nat Genet* 2000; **25**: 217-222.
32. Swick AG, Janicot M, Chenevalkastelic T, Mclenithan JC, Lane MD. Promoter cDNA-directed heterologous protein expression in Xenopus-laevis oocytes. *Proc Natl Acad Sci U S A* 1992; **89**: 1812-1816.
33. Vellinga J, van den Wollenberg DJM, Van der Heijdt S, Rabelink MJWE, Hoeben RC. The coiled-coil domain of the adenovirus type 5 protein IX is dispensable for capsid incorporation and thermostability. *J Virol* 2005; **79**: 3206-3210.
34. Wiertz EJHJ, Jones TR, Sun L, Bogyo M, Geuze HJ, Ploegh HL. The human cytomegalovirus US11 gene product dislocates MHC class I heavy chains from the endoplasmic reticulum to the cytosol. *Cell* 1996; **84**: 769-779.
35. Magnusson MK, Hong SS, Henning P, Boulanger P, Lindholm L. Genetic retargeting of adenovirus vectors: functionatity of targeting ligands and their influence on virus viability. *J Gene Medicine* 2002; **4**: 356-370.
36. Matthews QL, Sibley DA, Wu HJ, Li J, Stoff-Khalili MA, Waehler R, *et al.* Genetic incorporation of a herpes simplex virus type 1 thymidine kinase and firefly luciferase fusion into the adenovirus protein IX for functional display on the virion. *Mol Imaging* 2006; **5**: 510-519.
37. Vellinga J, Uil TG, de Vrij J, Rabelink MJWE, Lindholm L, Hoeben RC. A system for efficient generation of adenovirus protein IX-producing helper cell lines. *J Gene Medicine* 2006; **8**: 147-154.
38. Rosa-Calatrava M, Grave L, Puvion-Dutilleul F, Chatton B, Kedinger C. Functional analysis of adenovirus protein IX identifies domains involved in capsid stability, transcriptional activity, and nuclear reorganization. *J Virol* 2001; **75**: 7131-7141.

39. Davis MM, Boniface JJ, Reich Z, Lyons D, Hampl J, Arden B, *et al.* Ligand recognition by alpha beta T cell receptors. *Annu Rev Immunol* 1998; **16**: 523-544.
40. Norkin LC. Simian virus 40 infection via MHC class I molecules and caveolae. *Immunol Rev* 1999; **168**: 13-22.
41. Hong SS, Karayan L, Tournier J, Curiel DT, Boulanger PA. Adenovirus type 5 fiber knob binds to MHC class I alpha 2 domain at the surface of human epithelial and B lymphoblastoid cells. *EMBO J* 1997; **16**: 2294-2306.
42. Cattaneo A, Biocca S. The selection of intracellular antibodies. *Trends Biotechnol* 1999; **17**: 115-121.
43. Magnusson MK, Hong SS, Henning P, Boulanger P, Lindholm L. Genetic retargeting of adenovirus vectors: functionality of targeting ligands and their influence on virus viability. *J Gene Medicine* 2002; **4**: 356-370.
44. Magnusson MK, Henning P, Myhre S, Wikman M, Uil TG, Friedman M, *et al.* Adenovirus 5 vector genetically re-targeted by an affibody molecule with specificity for tumor antigen HER2/neu. *Cancer Gene Ther* 2007; **14**: 468-479.
45. Witlox MA, van Beusechem VW, Grill J, Haisma HJ, Schaap G, Bras J, *et al.* Epidermal growth factor receptor targeting enhances adenoviral vector based suicide gene therapy of osteosarcoma. *J Gene Medicine* 2002; **4**: 510-516.
46. Willemsen RA, Weijtens MEM, Ronteltap C, Eshhar Z, Gratama JW, Chames P, *et al.* Grafting primary human T lymphocytes with cancer-specific chimeric single chain and two chain TCR. *Gene Ther* 2000; **7**: 1369-1377.
47. van der Bruggen P, Traversari C, Chomez P, Lurquin C, De Plaen E, Van den Eynde BJ, *et al.* A gene encoding an antigen recognized by cytolytic T lymphocytes on a human melanoma. *Science* 1991; **254**: 1643-1647.
48. Fallaux FJ, Kranenburg O, Cramer SJ, Houweling A, VanOrmondt H, Hoeben RC, *et al.* Characterization of 911: A new helper cell line for the titration and propagation of early region 1-deleted adenoviral vectors. *Hum Gene Ther* 1996; **7**: 215-222.
49. Carlotti F, Bazuine M, Kekarainen T, Seppen J, Pognonec P, Maassen JA, *et al.* Lentiviral vectors efficiently transduce quiescent mature 3T3-L1 adipocytes. *Mol Ther* 2004; **9**: 209-217.
50. Barel MT, Pizzato N, van Leeuwen D, Le Bouteiller P, Wiertz EJHJ, Lenfant F. Amino acid composition of alpha 1/alpha 2 domains and cytoplasmic tail of MHC class I molecules determine their susceptibility to human cytomegalovirus US11-mediated down-regulation. *Eur J Immunol* 2003; **33**: 1707-1716.
51. Mittereder N, March KL, Trapnell BC. Evaluation of the concentration and bioactivity of adenovirus vectors for gene therapy. *J Virol* 1996; **70**: 7498-7509.
52. Caravokyri C, Leppard KN. Constitutive episomal expression of polypeptide-IX (pIX) in a 293-based cell-line complements the deficiency of pIX mutant Adenovirus type-5. *J Virol* 1995; **69**: 6627-6633.
53. Douglas JT, Rogers BE, Rosenfeld ME, Michael SI, Feng MZ, Curiel DT. Targeted gene delivery by tropism-modified adenoviral vectors. *Nat Biotechnol* 1996; **14**: 1574-1578.
54. Willemsen RA, Debets R, Hart E, Hoogenboom HR, Bolhuis RLH, Chames P. A phage display selected Fab fragment with MHC class I-restricted specificity for MAGE-A1 allows for retargeting of primary human T lymphocytes. *Gene Ther* 2001; **8**: 1601-1608.
55. Hsu KHL, Lonbergholm K, Alstein B, Crowell RL. A monoclonal-antibody specific for the cellular receptor for the Group-B Coxsackie-viruses. *J Virol* 1988; **62**: 1647-1652.